Real-Time Point-Positioning Performance Evaluation of Single-Frequency Receivers Using NASA's Global Differential GPS System

Ronald J. Muellerschoen, Byron Iijima, Robert Meyer, Yoaz Bar-Sever
Jet Propulsion Laboratory, California Institute of Technology

Elie Accad
Navigation and GPS Applications Department, Raytheon ITSS

Biography

Ron Muellerschoen received a B.S. degree in physics at Rensselaer Polytechnic Institute and a M.S. degree in applied math at the University of Southern California. He is currently a Senior Engineer in the Radar Science and Engineering Section at the Jet Propulsion Laboratory (JPL), California Institute of Technology. His work at JPL has concentrated on the development of filtering software for processing GPS data and the development of wide area differential systems. He was the lead architect in developing NASA's global differential GPS system.

Byron Iijima is a member of the Tracking Systems and Applications section at JPL. He primarily works on GPS techniques for remote sensing of the ionosphere and atmosphere, and their applications. He holds a Ph.D. in physics from MIT.

Robert Meyer works in JPL's Orbiter and Radiometric Systems Group developing RTG (Real-Time GIPSY) and IGDG (Internet-Based Global Differential GPS) for GPS and LEO orbit determination, time transfer and geodesy applications. His interests are in differential GPS, orbit determination, geodesy and time and frequency metrology for ground, airborne and space flight missions. He holds a BA, Physics from U.C. Santa Cruz.

Yoaz Bar-Sever is the Supervisor of the Orbiter and Radio Metric Systems group at JPL. He holds a Ph.D. in Applied Mathematics from the Technion - Israel Institute of technology (1987), and a Master in Electrical Engineering from the University of Southern California (1993). He joined JPL in 1989 where he has been involved in GPS technology development and its geophysical applications.

Elie Accad received a B.S. degree in aerospace engineering and a M.S. degree in applied math from the University of Southern California. He has previously worked on monitoring and analysis of the GLONASS constellation. Currently at Raytheon, he works with the GPS group at JPL on development and analysis of JPL's global differential system.

Abstract

This paper evaluates the real-time positioning performance of a single-frequency receiver using the 1-Hz differential corrections as provided by NASA's Global Differential GPS (GDGPS) System. While a dual-frequency user has the ability to eliminate the ionosphere error by taking a linear combination of observables, a single-frequency user must remove or calibrate this error by other means. To remove the ionosphere error we take advantage of the fact that the group delay in the range observable and the carrier phase advance have the same magnitude but are opposite in sign. A second way to remove this error is to calibrate the ionosphere with a real-time database of grid points computed by JPL's RTI (Real-Time Ionosphere) software. In both cases we evaluate the positional accuracy of a kinematic carrier phase based point-positioning method on a global extent.

Introduction

NASA's Global Differential GPS (GDGPS) System was developed to enable Earth-orbiting satellites, airplanes, and terrestrial users to achieve unprecedented levels of real-time positional accuracy with both seamless and global coverage. For kinematic applications, such as

airplanes and terrestrial vehicles, we have demonstrated sub decimeter-level accuracies worldwide [*Armatys, et al.,* 2003]. Additionally the system promises centimeter-level accuracy for applications with largely predictable dynamics, such as satellites in Earth orbit.

The GDGPS system is focused toward users with dual-frequency receivers that are prevalent in scientific and high-end applications. Dual frequency users can eliminate ionosphere errors by taking a linear combination of observables. The errors in the GPS ephemerides and GPS clocks are provided to the user by a 1-Hz GDGPS correction message. This correction message is transmitted to the user as a signal-in-space (SIS) or can be accessed over the Internet if available. For slowly moving ground-based users, troposphere errors can be accounted for by estimating a time-varying zenith troposphere parameter. For aircraft users at altitude, barometric pressure observations are sufficient to model the dry component of the troposphere delay [*Muellerschoen et al.*, 1999].

Single-frequency receivers have the advantage that they are low-cost and the CA-code acquisition for civilian access provides higher signal to noise ratio than a synthesized P-code acquisition. We investigate techniques for extending the use of the GDGPS correction message to single frequency users.

System Overview

Accurate global corrections to the broadcasted GPS ephemerides and GPS clocks are computed from a global network of GPS reference sites. We use NASA's Global GPS Network (GGN), which is operated and maintained by JPL. To return data in real-time, a new software set called Real-Time Net Transfer (RTNT) was developed. One Hertz phase and range observables are returned over the Internet using User Datagram Protocol (UDP). More than 98% of the data is returned in less than 2 seconds from sites with good Internet connections. Currently 40 GGN sites are returning data in real-time to JPL (Fig. 1). The real-time performance and latency of all the stations in this network can be monitored at http://gipsy.jpl.nasa.gov/igdg/demo/.

The fundamental tenet of our architecture is a *state-space* approach, where the orbits of the GPS satellites are precisely modeled, and the primary estimated parameters are the satellite states and clocks. Since we are estimating real physical parameters, this approach guarantees that the corrections will be globally and uniformly valid. In contrast, most differential systems employ a *measurement* approach, where the estimated parameters are range corrections. In the measurement approach, positioning error is dependent on the user's location relative to the reference network.

Additional information on the real-time GPS clock and orbit determination processes, including estimation of Earth orientation parameters can be found in [*Muellerschoen et al.*, 2000] and [*Muellerschoen et al.,* 2001]. On-line information is available at http://www.gdgps.net

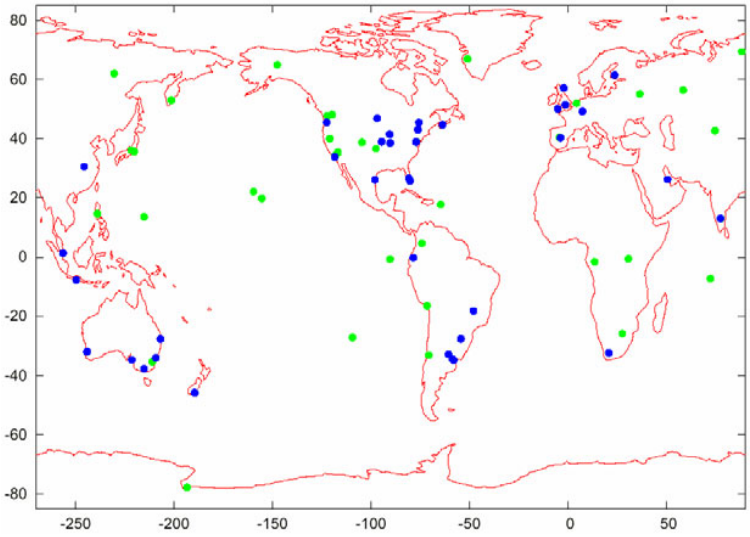

Fig. 1) Network of dual-frequency GPS reference receivers returning data to JPL in real-time. The green dots indicate GGN sites while the blue dots indicate other agency data sites. There is some overlap of sites that may be hidden in the above.

Operations are automated and performed redundantly at two processing centers. To support continuous and reliable operations, these processing centers are set up in a secure environment. The centers are configured with multiply redundant computers, and backed up by uninterruptible power supplies.

Communicating the Corrections

The differential corrections produced at the central processing center are optimally packed to allow for efficient relay to the users. The SIS corrections are packaged into a 28-byte/second message. Each one-second message contains xyz orbit and velocity corrections for one PRN, and clock corrections for 16

PRNs. Clock corrections for a second set of 16 PRNs are transmitted on alternating seconds. IODE ephemeris changes are held 2 minutes after new IODEs are observed. This allows the user sufficient time to accumulate the newest broadcast ephemeris message.

The global differential corrections are also available over the Internet or dedicated lines via either a TCP or UDP server running at the operation centers. Figure 2 represents a 24-hour plot of a non-moving user of a receiver at the Alternative Master clock in Colorado Springs, Colorado, US with the global correction message. The RMS user errors are 4, 3, and 6 cm in east, north, and vertical, respectively. Ongoing demonstrations can be additionally found at http://gipsy.jpl.nasa.gov/igdg/all_demos/.

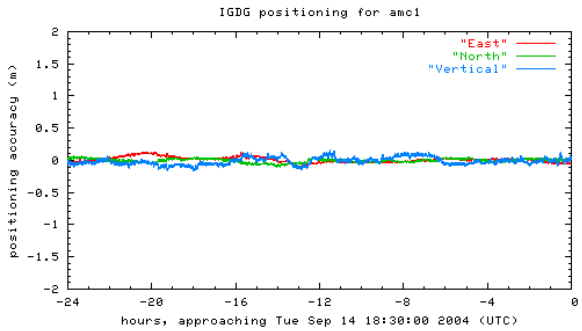

Fig. 2) 24-hour one Hertz user position error of a dual-frequency receiver with kinematic positioning using the global differential corrections.

Table 1 presents a sampling of sites from the global network. Dual-frequency kinematic root-mean-square horizontal errors are typically better than 10 cm in the horizontal and better than 15 cm in the vertical.

Site Location	RMS Error East (cm)	RMS Error North (cm)	RMS Error Up (cm)
Urals Ridge, Russia	3	3	6
Colorado Springs, CO	4	3	6
Brewster, WA	5	3	9
Delft, Holland	4	4	10
Fairbanks, AK	9	7	13
Krugersdorp, S. Africa	4	3	8
Bangalore, India	8	5	9
Madrid, Spain	5	3	11
Tidbinbilla, Australia	4	5	10

Table 1) 24-hour one Hertz user position error of a global distribution of dual-frequency receivers with kinematic positioning using the global differential corrections.

Eliminating the Ionosphere

Method 1, GRAPHIC Data Type

The GRAPHIC observable (Group and Phase Ionosphere Calibration [*Gold et al.,* 1994] takes advantage of the fact that the group delay in range observable and the carrier phase advance have the same magnitude but are opposite in sign.

The L1 phase and P1 range observables can be modeled as:

$$L_1 = \rho - \mathrm{I} + \lambda_1 b_1 + \phi + \eta_\varphi + B_1 \quad (1)$$

$$P_1 = \rho + \mathrm{I} + \eta_R + B_1 \quad (2)$$

where

ρ non-dispersive delay

I ionosphere at L1 frequency

λ_1 L1 wavelength $\approx$ 19.0 cm

b_1 phase bias (non integer)

η_φ phase noise $\approx$ few mms.

η_R range noise + multipath $\approx$ few meters

ϕ phase windup

B_1 interfrequency bias at L_1

B_2 interfrequency bias at L_2

where

$$\tau_{gd} = \frac{f_2^2}{f_1^2 - f_2^2}(B_2 - B_1) \approx 1.54(B_2 - B_1)$$

f_1 L1 frequency at 1.57542 GHz

f_2 L2 frequency at 1.22760 GHz

The non-dispersive delay lumps together the effects of geometric and troposphere delays, and both GPS and receiver clock errors. The phase windup accounts for the phase accumulation of the GPS right-hand circularly polarized (RCHP) wave front as the relative antenna rotation changes between the GPS transmitter and receiver.

The average of L1 (less the modeled phase windup) and P1 provides a biased range observable, analogous to the phase measurement but with noise equivalent to one-half that of single frequency range data. To reduce the noise on this synthesized data type we smooth the carrier with the range. That is, we construct L_G as:

$$L_g(t) = L_1(t) + \frac{1}{2}\langle P_1 - L_1 \rangle \qquad (3)$$

$$= \rho(t) + \frac{\lambda_1 b_1}{2} + \left(\langle I \rangle - I(t)\right) + \frac{\langle \eta_R \rangle}{2}$$

$$+ \phi(t) + \eta_\varphi(t) - \frac{\langle \eta\varphi \rangle}{2} + B_1$$

$$\approx \rho + \frac{\lambda_1 b_1}{2} + \phi + \eta_\varphi + B_1$$

$$+ \varepsilon(Ionfit) + \varepsilon(Multipath)$$

where < … > indicates a **linear** fit to the last N 1-Hz data points and

$$\varepsilon(Ionfit) = \left(\langle I \rangle - I(t)\right) \qquad (4)$$

$$\varepsilon(Multipath) = \frac{\langle \eta_R \rangle}{2} \qquad (5)$$

Equation 3 is very similar to the first expression for L_1 (eq. 1) without the ionosphere term I, but with errors due to the ionosphere fit and P1 multipath. Note that in constructing this observable there is a tradeoff between how the ionosphere at time t can be estimated by a linear fit from the Nth point interval and how much multipath reduction can be achieved. The longer the interval, the more averaging of the multipath, however more error in the ionosphere fit to time t. In this paper we do not consider higher order fits since they tend to chase multipath signatures rather than reduce noise. We did attempt quadratic fits, but this resulted in substantial worse performance.

We can determine the error due to the linear fit of the ionosphere with the true ionosphere if we have a collocated dual frequency receiver at the site. In fact we use a dual frequency receiver and for the results presented in this paper, we use the P1/L1 data. Since

$$L_2 = \rho - \frac{f_1^2}{f_2^2} I + \lambda_2 b_2 + \phi + \eta_\varphi + B_2 \qquad (6)$$

we can compute the actual ionosphere as

$$L_1 - L_2 = \frac{f_2^2}{f_1^2 - f_2^2} \mathrm{I} + \text{ other} \qquad (7)$$

$$\approx \frac{1}{1.54} \mathrm{I} + \text{other}$$

where "other" includes constant terms, small noise terms, or slowing changing phase windup.

We compute an N point linear fit to L1-L2 and compare the predicted value to L1-L2 at the next second. We then take the root-mean-square of these differences over a pass and multiply by 1.54 according to eq. 7.

To determine the multipath contribution, we compute the scatter in the N point means of

$$P_1 - L_1 - \frac{2 f_2^2}{f_1^2 - f_2^2}(L_1 - L_2) \qquad (8)$$

and divide by 2 according to eq. 5.

Figures 3 and 4 show the results of the increasing ionosphere errors in the fit and the decreasing multipath contribution as the size of the fit (N) is increased from near 0 to 3600 seconds. Optimally we select N where the root-sum-of-squares of these two is minimal. From the results, a value of 1000 appears to be an optimal selection of N for this particular site.

These data were generated from a dual frequency Dorne Margolin antenna with a choke ring at JPL (34 degrees North latitude). Data for other sites has not been generated but it would be expected that N could be optimally selected based on both ionosphere conditions and antenna type.

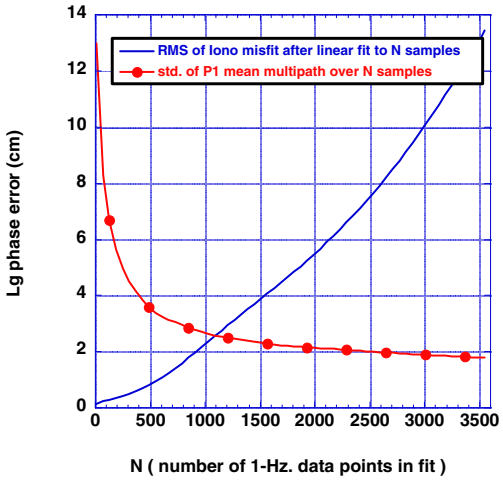

Fig. 3) Ionosphere error contribution (eq. 4) and multipath error contribution (eq. 5) to GPS15 Lg observables as a function of fit size.

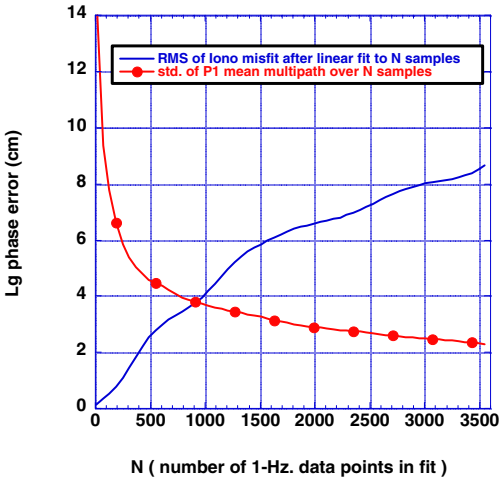

Fig. 4) Ionosphere error contribution (eq. 4) and multipath error contribution (eq. 5) to GPS17 Lg observables as a function of fit size.

Method 2, Real-Time Iono Grid points.

An alternative method of removing ionosphere delay from single-frequency GPS data uses a database of global grid maps of ionosphere electron density. These maps are created in real-time using JPL's Real-Time Ionosphere

(RTI) algorithm, taking as input data from the GDGPS network of GPS receiver. These maps are estimated every minute with a latency of less than 10 seconds. Since the GDGPS GPS receivers are dual-frequency, they provide measurements of line-of-sight integrated electron content (TEC) for each link between the receivers and the GPS satellites.

The value of ionosphere content at the grid points is computed using a Kalman filter. Climatological data and the relative stationarity of the electron content in the solar-magnetic frame are used in the filter to help extrapolate the maps where data coverage is poor. The filter also produces values for the inter-frequency group delay biases of the GPS satellites and for the GPS receivers.

Real-time maps generated by RTI using the GDGPS data are currently displayed on
http://iono.jpl.nasa.gov/latest_rti_global.html

The accuracy of the ionosphere delay computed from the real-time grid maps can be assessed by comparing slant range TEC with post-processed data from a more complete global distribution of dual-frequency receivers. Figure 5 shows the R.M.S. values for the difference between the post-processed global ionosphere delay and grid values generated by RTI. RTI models the ionosphere as a thin shell of electrons at 450 km altitude. [*Mannucci et al.*, 1998]. The electron concentration on the global shell was parameterized using 642 grid points, which were vertices of a uniform triangular tiling of the shell. The electron content varies linearly among the grid points.

RTI performs best where the ionosphere is relatively smooth in space and time, and where data from the real-time network is available. RTI performance degrades in areas where data is sparse and where the ionosphere has larger spatial and temporal structure such as at low magnetic latitudes and during the afternoon local time, or during geomagnetic disturbances. For example, at latitudes > 30 degrees, the R.M.S. accuracy is better than 1 meter. On the other hand at lower latitudes, the ionosphere correctors can be highly inaccurate due to large gaps in the real-time sites and the high spatial/temporal variability of the ionosphere at those latitudes.

More sophisticated ionosphere models than the one used in this test (e.g. 3-dimensional models and physics-driven data assimilation models) can also be used [*Hajj et al.*, 2004]. These models have not been evaluated for single frequency receiver navigation performance.

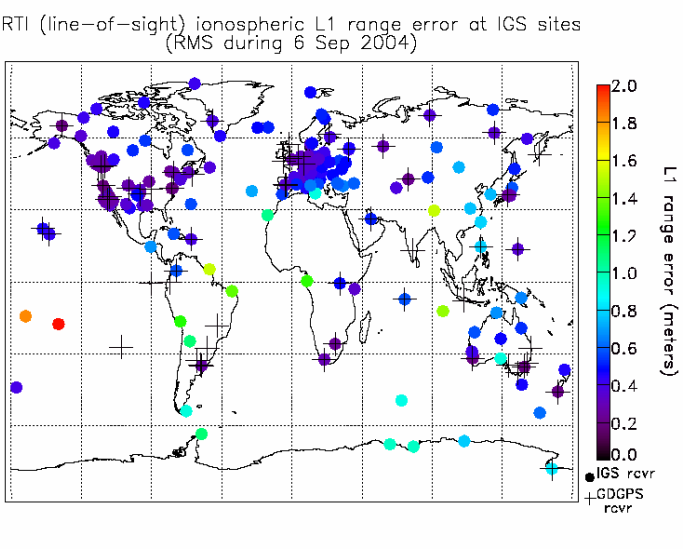

Fig. 5) 24-hour TEC slant range R.M.S. of Real-Time Ionosphere as compared with a more globally complete post-processed solution. Sites with a "+" were used in the RTI estimation. Scale is from 0 to 2 meters range error at L1. Most of North America and Europe range errors are better then 0.5 meters.

GRAPHIC Results

To test the accuracy of the GRAPHIC method, kinematic point-positioning runs for a number of geographically distributed sites were performed. The table 2 below shows results obtained for sites over a period of 6 days, from August 10th, to August 16th, 2004, using an elevation mask angle of 9°. The Lg data type was weighted at 10 cm with no de-weighting for low elevations.

Site Location	RMS Error East (cm)	RMS Error North (cm)	RMS Error Up (cm)
Urals Ridge, Russia	15	16	22
Colorado Springs, CO	12	10	34
Brewster, WA	12	17	31
Delft, Holland	9	9	22
Fairbanks, AK	19	16	39

Krugersdorp, S. Africa	13	10	26
Bangalore, India	16	12	41
Kokee Park, HI	11	9	24
Madrid, Spain	21	33	32
Singapore	17	11	33
Tidbinbilla, Australia	8	7	20

Table 2) Six day R.M.S. results of one Hertz user position error of a global distribution of single-frequency receivers with kinematic positioning using the global differential corrections and the modified GRAPHIC data observable formulated to reduce receiver multipath.

Combining the results for all the sites, the GRAPHIC method yielded RMS user errors of 14, 15 and 30 cm in east, north and vertical, respectively. This translates into a 3-dimensional RSS error of 36 cm, which is about 3 times worse than the performance obtained with dual-frequency point-positioning.

Startup of GRAPHIC Positioning

A point-positioning run is started in static mode to allow the solution to settle quickly. After ten minutes, the solution switches to kinematic mode. Figure 6 shows the settling time for a single-frequency point-positioning run for a site in Singapore. The behavior illustrated in the plot below is representative of the single-frequency runs that were performed.

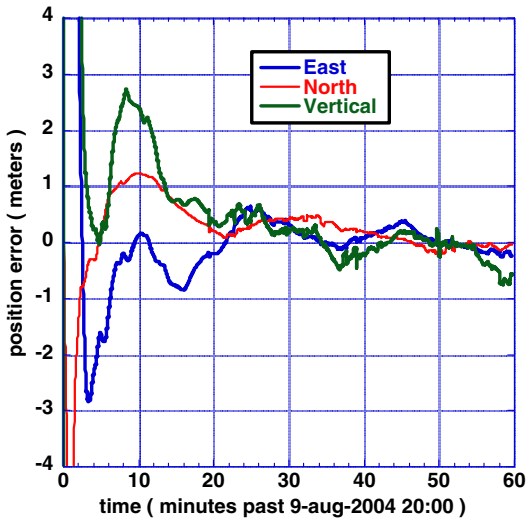

Fig. 6) Single-frequency GRAPHIC settling errors for a receiver in Singapore. After 10 minutes the filter switches from static to kinematic mode.

RTI Results

To test the accuracy of the RTI method, kinematic point-positioning runs for a few number of geographically distributed sites were performed. Figures 7, 8, and 9 show results obtained for JPL Mesa, California, US, Madrid Spain, and Tidbinbilla Australia. The 3-D RSS error for JPL Mesa was 48 cm, and for both Madrid and Tidbinbilla 64 cm. In generally the results are about a factor of 2 worse than the performance obtained with the GRAPHIC approach.

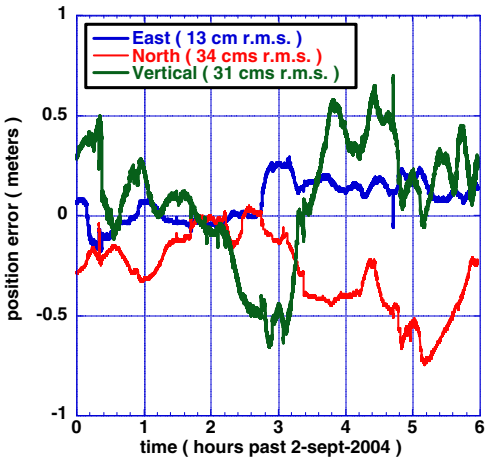

Fig. 7) single freq. results from JPL Mesa using RTI

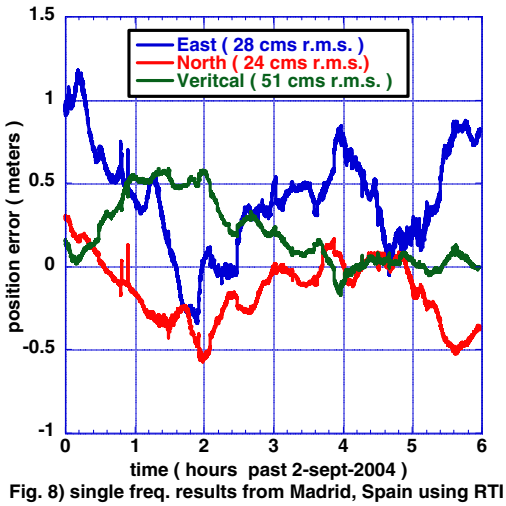

Fig. 8) single freq. results from Madrid, Spain using RTI

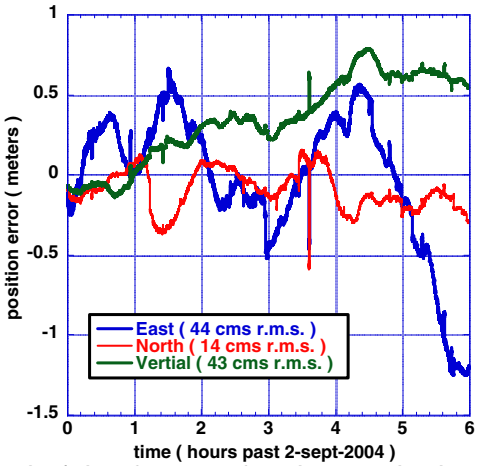

Fig. 9) single freq. results from Tidb. Australia using RTI

Summary

The extension of NASA's global differential GPS corrections to single-frequency users using a modified version of the GRAPHIC data type formulated to reduce receiver multipath gives a 3-D RSS error of 36 cms evaluated on a global scale. This is about 3 times worse than a typical dual-frequency user. Real-Time Ionosphere (RTI) kinematic positioning results are typically 2 to 3 times worse than these with the modified GRAPHIC positioning errors.

Acknowledgments

The work described in this paper was carried out in part by the Jet Propulsion Laboratory, California Institute of Technology, under contract with the National Aeronautics and Space Administration.

Part of the work presented in this paper was performed at Raytheon under a contract with the Jet Propulsion Laboratory, California Institute of Technology, under a contract with the National Aeronautics and Space Administration.

References

Armatys, M., Muellerschoen, R,J., Bar-Sever, Meyer, Demonstration of Decimeter-level Real-time Positioning of an Airborne Platform, Proceedings of ION NTM-2003, Anaheim, California, January 2003.

Gold, K., W. I. Bertiger, S. C. Wu, T. P. Yunck, GPS Orbit Determination for the Extreme Ultraviolet Explorer, *Navigation: Journal of the Institute of Navigation*, Vol. 41, No. 3, Fall 1994, pp. 337-351

Hajj, G. A., B. D. Wilson, C. Wang, X. Pi, I. G. Rosen, Data assimilation of ground GPS total electron content into a physics-based ionospheric model by use of the Kalman filter, *Radio Science*, Vol. 39, RS1S05, doi:10.1029/2002RS002859, 2004.

Mannucci, A.J., B. D. Wilson, D. N. Yuan, C. H. Ho, U. J. Lindqwister, T. F. Runge, "A global mapping technique for GPS-derived ionospheric total electron content measurements," *Radio Science*, Volume 33, Number 3, pp 565-582, May-June 1998

Muellerschoen, R. J., W. I. Bertiger, Flight Tests Demonstrate Sub 50 cm RMS. Vertical WADGPS Positioning, Proceedings of ION GPS-99, Nashville, Tenn. September 1999.

Muellerschoen, R. J., W. I. Bertiger, M. F. Lough, Results of an Internet-Based Dual-Frequency Global Differential GPS System, Proceedings of IAIN World Congress, San Diego, California, June, 2000.

Muellerschoen, R.J., A. Reichert, D. Kuang, M. Heflin, W.I. Bertiger, Orbit Determination with NASA's High Accuracy Real-Time Global Differential GPS System, Proceedings of ION GPS-2001, Salt Lake City, Utah, September 2001.